miRoot TUTORIAL 1.0

To facilitate single-cell exploration of the root-tip's miRNA biology, the F:AGO1-IP and F:RPL18-IP sequencing data-sets were integrated into a user-friendly browser coined miRoot, designed to operate on desk computers, tablets or smartphones. Cell-specific signals for single miRNAs (WT background) or single mRNA translatomes (WT/*hyl1-2* backgrounds) are queried in miRoot via a virtual root interface where colored patterns of various intensities reflect the relative pan-layer signals' strengths expressed in absolute or log2 values. The interface was designed by graphic cell layer deconvolution based upon authentic high-resolution photographs of WT versus *hyl1-2* root tips, as depicted in (**A**).

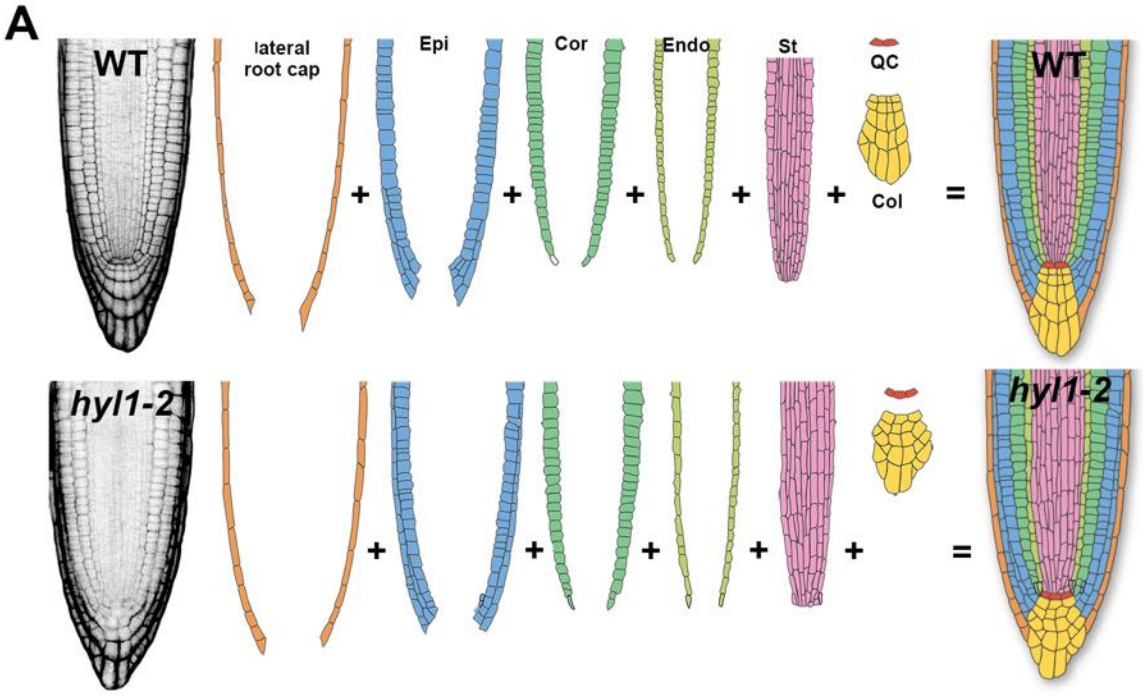

The virtual root depictions therefore take into account the characteristics of *hyl1-2* compared to WT root-tips, including cellularly disorganized columella and quiescent center (QC), enlarged stele, and defects in the anticlinal-*versus*-periclinal division rates of epidermal cells. The layers were then digitalized and assembled to reconstitute the

virtual root interfaces. Note that we were unable to isolate F:AGO1 at sufficient levels using the QC-specific *WOX5* promoter (Ref), presumably because the QC is made up of only four cells. The *SCR::GFP* (endodermis) signal overlaps the QC in the post-embryonic root (Ref2) and was indeed used, in previous FACS-based studies, to encompass the QC transcriptome and total sRNAome (Ref1, Ref2). While the same approximation could be made here, we nonetheless treated the QC as an unexplored layer for the sake of data accuracy.

● In the **miRNA-query** miRoot setting shown in **B** (blue square on the top), all currently known Arabidopsis miRNAs (miRbase v.21) may be interrogated primarily via their numeric identifier. Upon miRNA query, all known matching miR-5p/3p and paralogs (a, b, c, d…) are displayed in a pulldown menu alongside the sequence of the mature miRNA guide strand (blue rectangle):

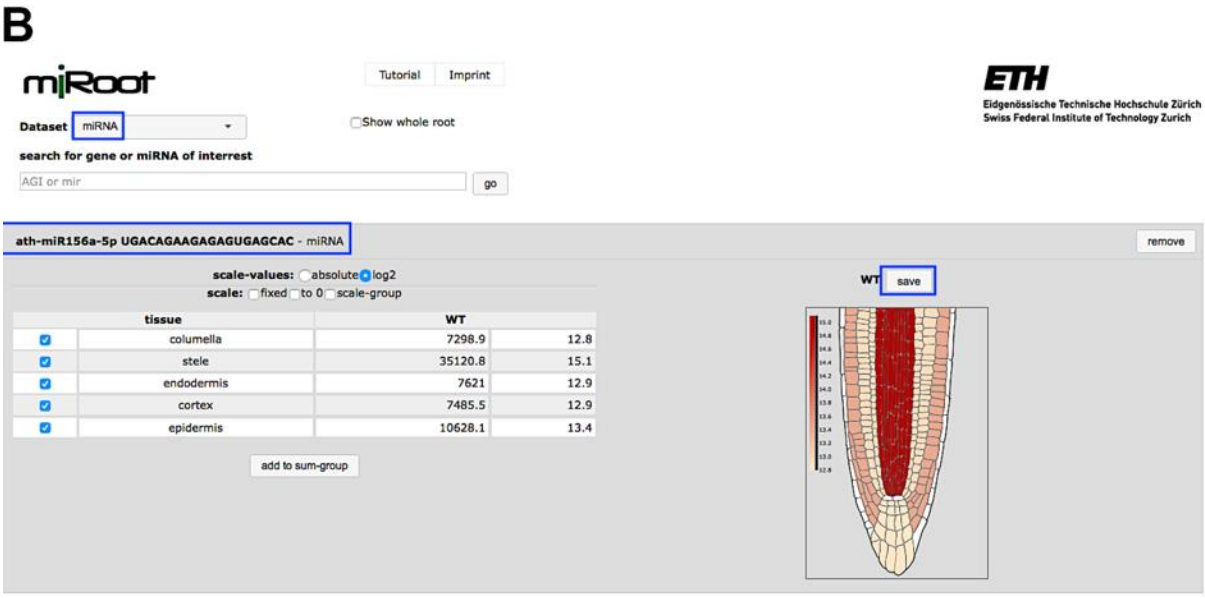

We stress that miRoot displays signal intensities for AGO-loaded *i.e.* functional miRNAs, that are relative to one another between cell layers. The cross-layer signals of the miR156 isoform **a,** strand **5p** are depicted here as an example. Root images are

exported in an Adobe Illustrator® CS6-compatible format via the save option (blue square).

● In the **transcript-query** miRoot setting shown in **C** (blue square on the top), the full, curated Arabidopsis transcriptome (TAIR10) may be interrogated via gene identification number (e.g. *AT1G69170* here), gene describer (e.g. SBP-domain transcription factor) or gene name (e.g. *SPL6*). In its most simplified implement, miRoot can thus be used as a root-tip layer-specific translatome analyzer. We have verified that its performances are at least on par with those of the cell-specific root translatome available from the eFP bowser (Bailey-Serres group at UC Riverside, USA).

C

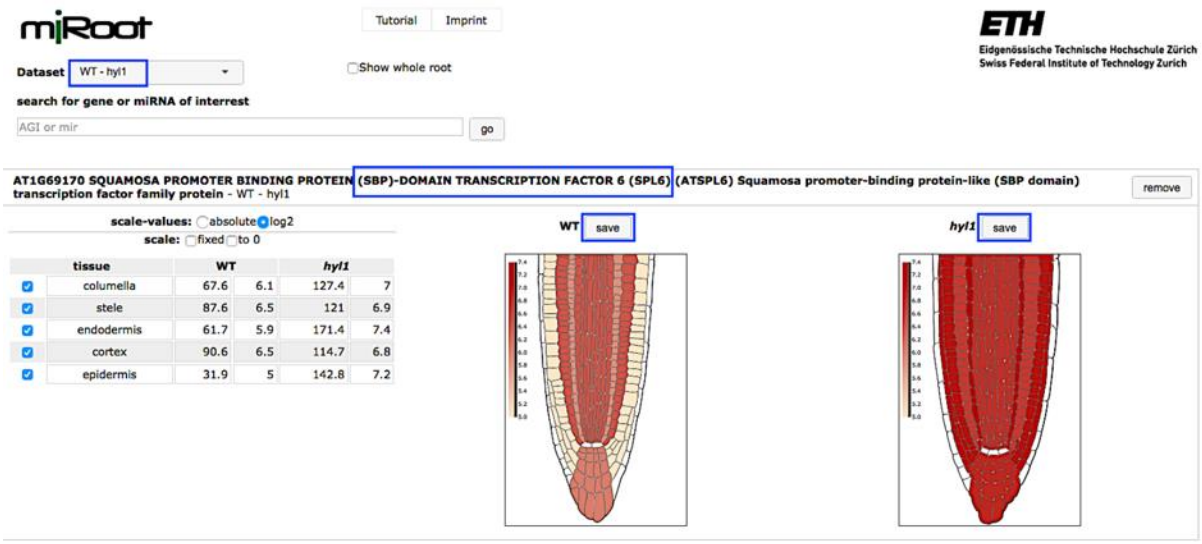

All plant miRNA targets predicted and/or validated so far display extended miRNA:target site complementarity such that they constitute a highly predictable subset of the Arabidopsis transcriptome. In the example shown in (**C**) the miR156 target *SPL6*^{miR156} was queried and thus can be compared visually with the colored maps obtained in (**B**) for the miR156**a**. Here, mutually-exclusive patterns of AGO1-loaded miR156a, on the one hand, and *SPL6*^{mir156} accumulation on the other, are

observed, as expected from a direct, cell-autonomous plant miRNA-target interaction. Note that the stele signals do not show, however, this mutually-exclusive pattern and this will be addressed in points **F**-onward.

- miR156 belongs to an extended family of paralogs (**a-b-c-d-e-f-g-h-i**) displaying each single-nucleotide polymorphisms that may refine targeting of specific *SPL* transcripts. Some of these paralogs are much less expressed and loaded into AGO1 than others, however, yet miRoot will display layer-specific patterns regardless of signal intensity. This might be confusing when visually analyzing the respective contributions of isoforms to target regulation as illustrated in panel (**D**) with miR156**a** signal and miR156**g**. The raw values (squared in blue) show that the signal intensity for paralog **a** is two-orders-of magnitude higher than that of paralog **g**.

D

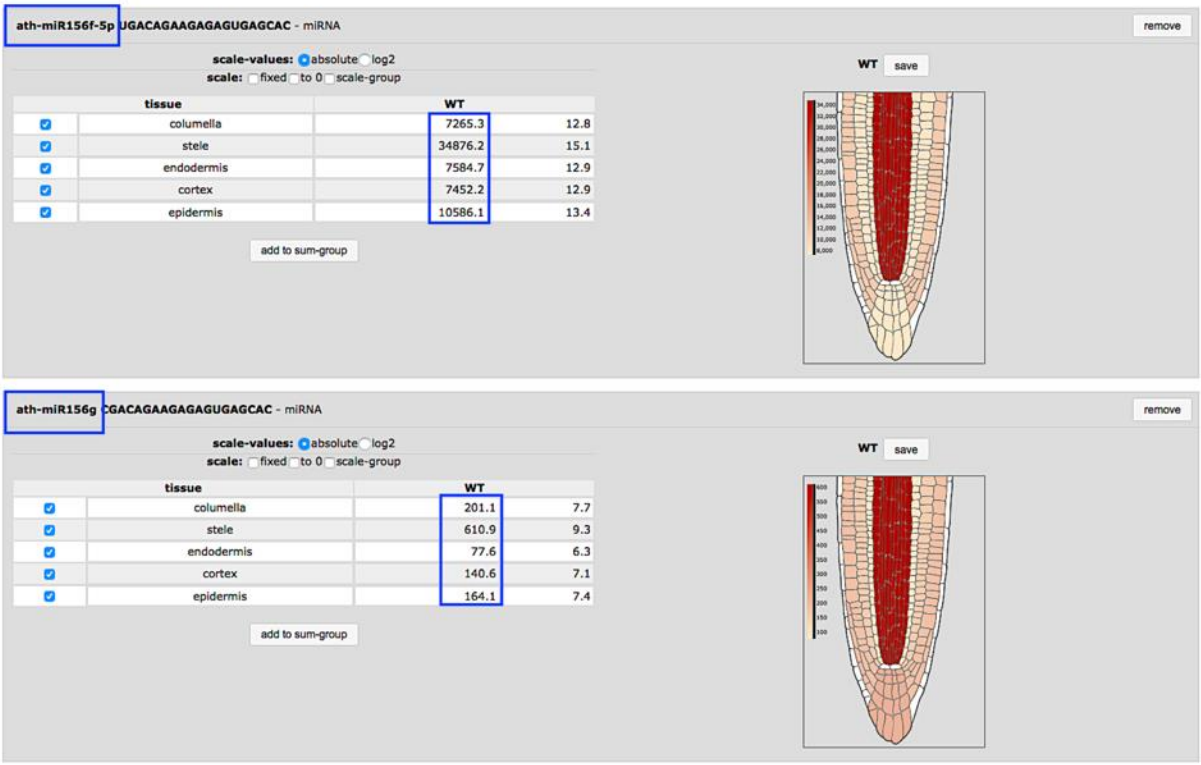

● The scale option (panel **E**, blue square and inlay) solves this issue by allowing signal normalization between any number of miRNA paralogs subjected to the option, with the values being recalculated relative to the paralog displaying the highest-intensity signal. Panel (**E**) bellow illustrates how rescaling highlights the near-background AGO1-loading signal of miR156 paralog **g** across root cell layers. Signal rescaling of all miR156 paralogs likewise identified that, in addition to **g**, paralogs **h** and **l** have no significant contribution to root-tip gene regulation (not shown). miR156 paralogs **a-b-c-d-e-f-g** display similar AGO1-loading signals in each root-tip layer, and since they are all involved, in principle, transcript targeting, it might be desirable to measure their bulk contribution to *SPL6*^{miR156} regulation in each cell layer.

E

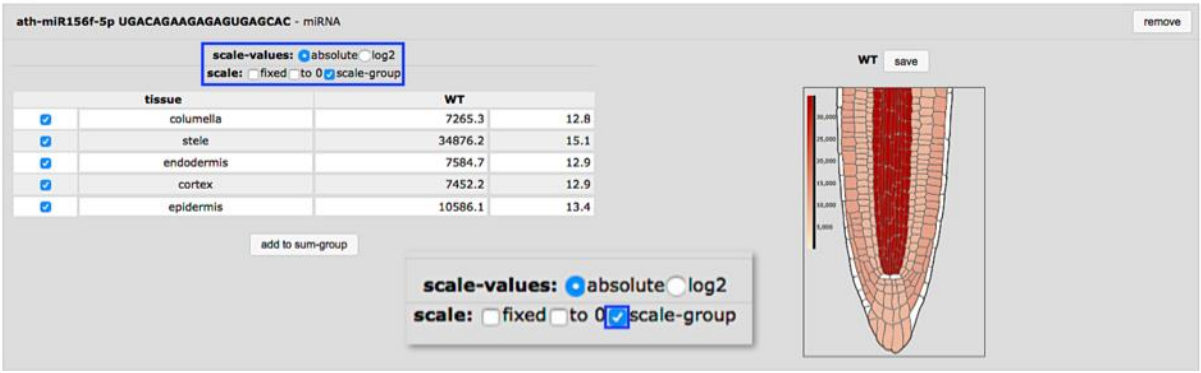

● As shown in (**F**) miRoot allows signal accretion via the “add to sum-group” option (the blue rectangle shows that any miRNA paralog can be selectively removed from the sum-group at any time). A “Sum-Group” is then generated (blue rectangle, top right corner) upon which the “create” option allows signal aggregation in each individual layer, as depicted here in the grey zone for miR156**a-b-c-d-e-f-g**. Note that signal accretion can also be useful to reconstitute the inferred bulk regulation conferred by paralogous miRNA displaying distinct spatial AGO1-loading patterns and/or different

signal intensities. It was used, for instance, in the source publication, with miR164**a/b** and miR164**c** (Figure S10C).

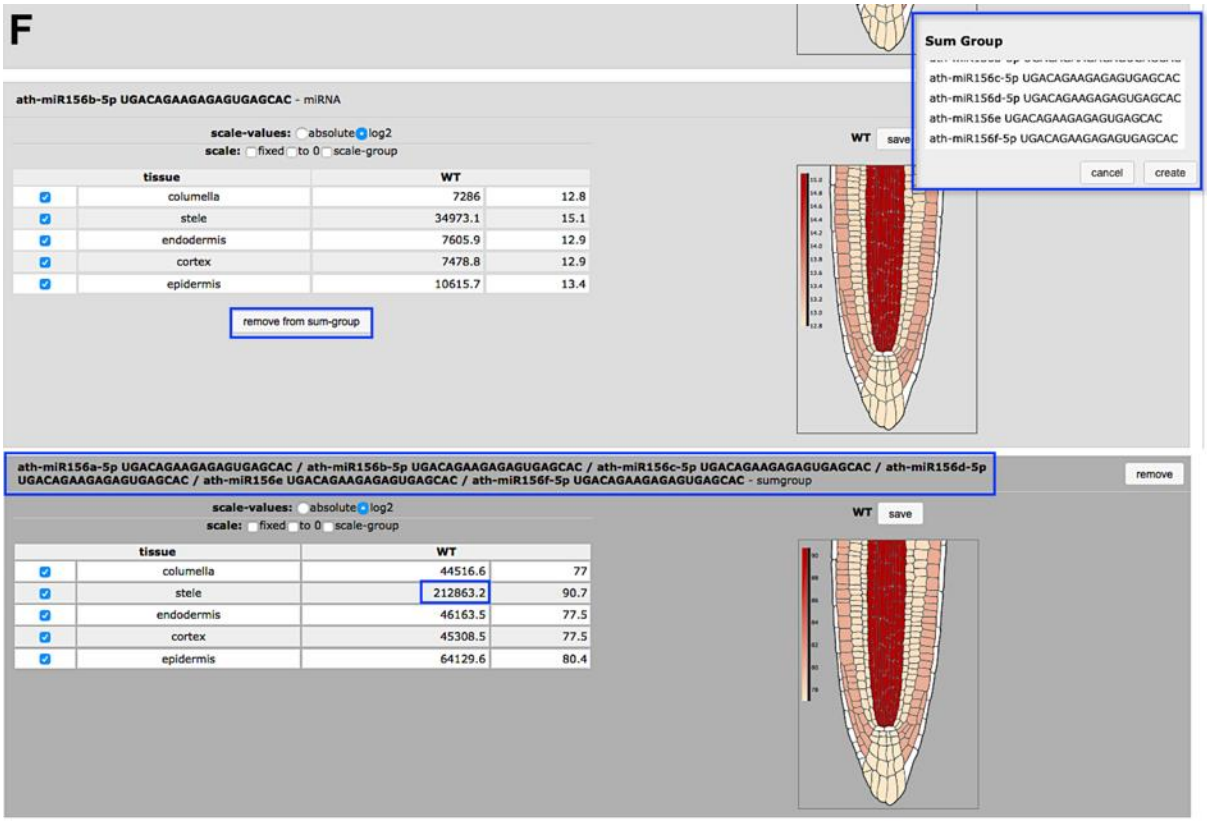

● Importantly, miRoot also enables removal of single/multiple layers and concurrent re-calculation of relative signal intensities across the remaining cell files. This option notably enables exclusion of the stele, of which none of the four intrinsic layers was individually resolved by *SHR*:F::AGO1-IPs because the *SHR* promoter is stele-generic. miRoot will thus artificially assign often elevated and single-layer signals to the other stele layers. Because the stele represents a major fraction of the root, this can create exaggerated signals potentially masking/undermining those of adjacent cell files, since all signals are relative to each-others. (**F-G**) illustrate this phenomenon with elevated stele-derived signals from each miR156 paralogs **a-f** (~35,000 normalized read couts/paralog, panel B) resulting, upon accretion, in a total signal of ~213,000

normalized read counts (panel F, blue square). As shown in **(G,** blue rectangle), these elevated signals barely contribute to *SPL6*^{mir156} transcript regulation in the whole stele (1.3 folds-change in *hyl1* versus WT).

G

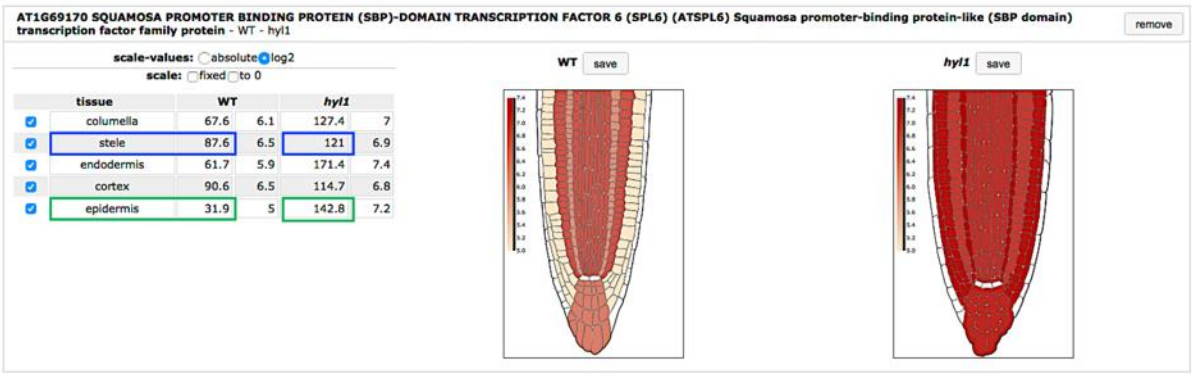

Accordingly, no significant change in *SPL6*^{mir156} accumulation is observed in the stele in the WT compared to *hyl1* backgrounds (**C**). This suggests that the strong stele miR156 signals originate mainly from a single, as yet undefined stele cell-type, and are diluted in the others. By contrast, for instance, the epidermis-derived miR156**a-f** signals (green square), contribute significantly to *SPL6*^{mir156} control in this layer, given the 4.5 folds-change in *hyl1* versus WT transcript accumulation observed (**G**).

● Panel (**H-I**) shows how the stele removal option used on both the miR156**a-f** (**H**) and *SPL6*^{mir156} (**I**) miRoot outputs resolves the caveat and provides, upon recalculation of relative signal intensities across all adjacent layers, a more accurate view of the spatial *SPL6*^{mir156} regulation. In particular, the epidermal miR156 **a-f** pool now clearly stands out as the dominant contributor to this spatial regulation (compare **B-C** to **H-I**). These adjustments thereby contribute to refine the mutually-exclusive pattern observed initially (**B-C**). As expected, the *SPL6*^{mir156} translatome signal is elevated in all layers in the *hyl1* background, and in the epidermis in particular. This optional layer-removal

feature is also useful to focus analyses of layer-specific regulations, as was done in the case of *GRF2* regulation by miR396a in Figure 3H-J of the source publication.

H

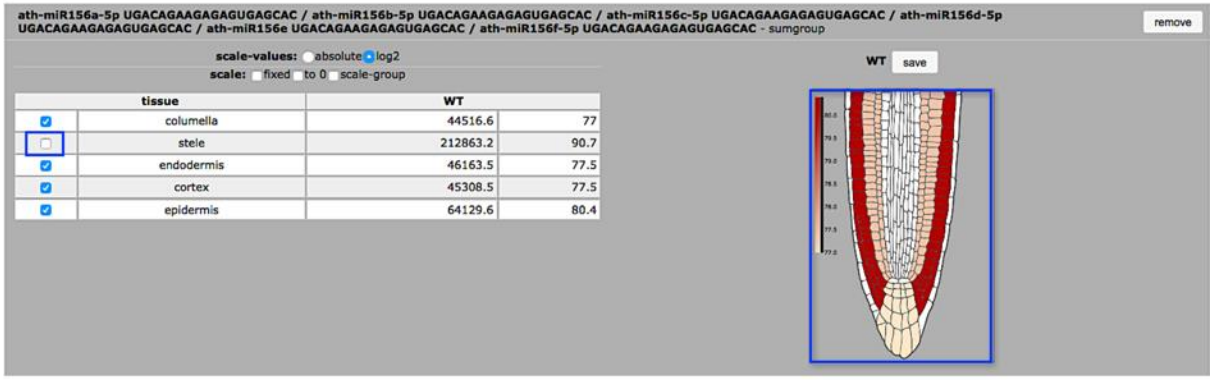

I

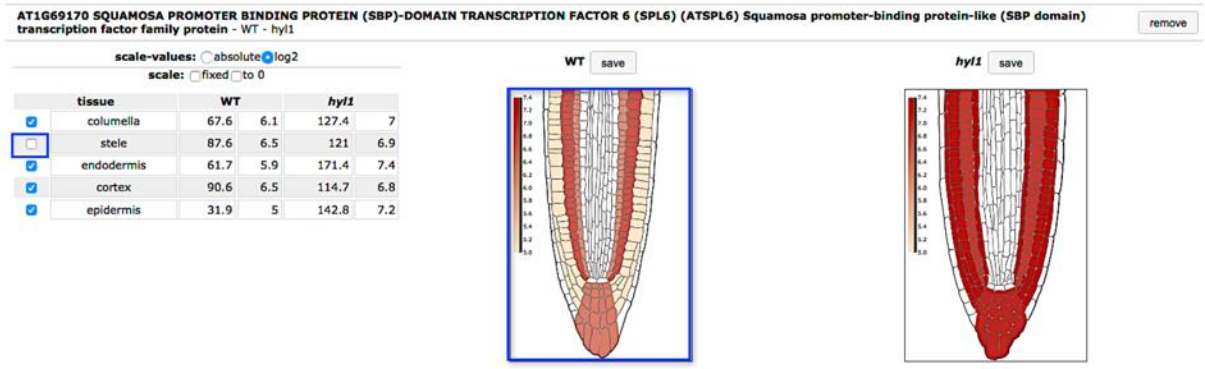

We hope you will find miRoot useful in exploring miRNA:target gene regulations in the Arabidopsis root tip. Note that the plethora of new miRNAs discovered in the source publication, their isomiRs and targets thereof will be incorporated shortly in a new version of miRoot, once the new data deposition process is completed.

Your questions, comments, suggestions or critics are welcome at miroot@impb.biol.ethz.ch and we will do our best to address them as soon as possible.